



Deep Ultraviolet Pre-Resonance Raman Scatter of Ice and Its Implications for Climate Research



Ryan R. Neely III[†], C. Todd Chadwick[†], Adam Willitsford[‡], Russell Philbrick[‡], Hans Hallen[†]

[†] Department of Physics, North Carolina State University [‡] Department of Electrical & Comp. Eng., Pennsylvania State University

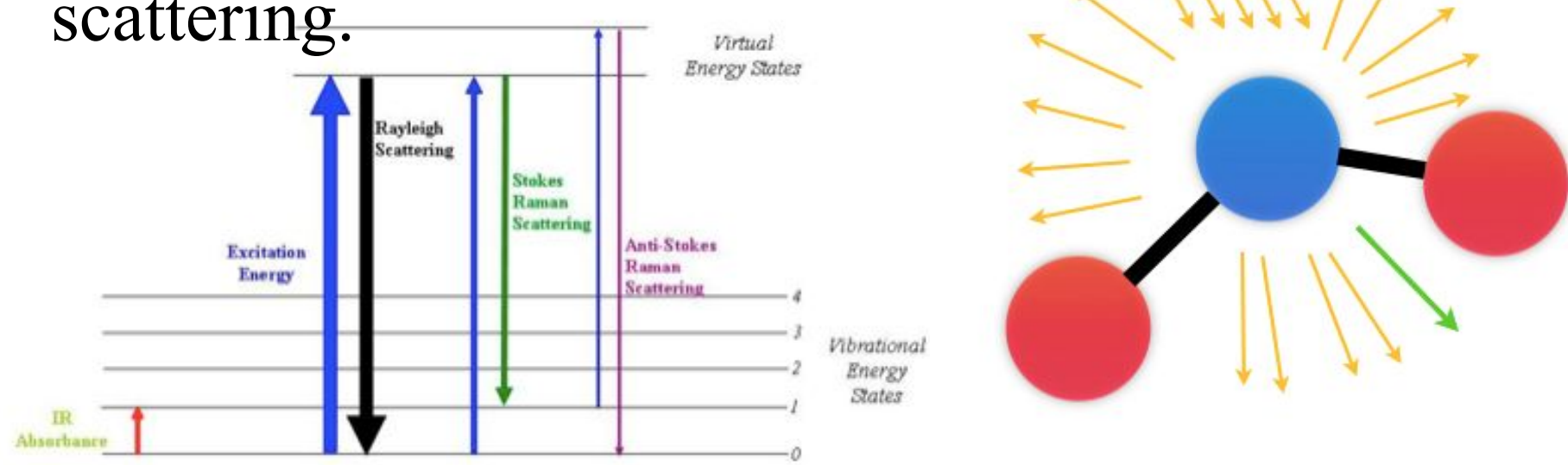
Abstract

The Raman scattering of ice has been investigated near the first deep ultraviolet electronic absorption. As the excitation beam approached the absorption band of water, significant enhancement in the Raman signal was observed. After normalizing for the non-resonant dipole absorption/radiation effects and input laser power, the integrated intensities of the Raman spectra for excitation energies ranging from 2.9eV to 5.6eV were compared. The A term of the Raman scattering tensor, which describes the pre-resonant enhancement of the spectra, models the observed intensities as a function of incident beam energy. These findings suggest that application of pre-resonant or resonant Raman LIDAR could vastly improve spatial and temporal resolution of water vapor measurements in clouds.

Theory

- Light can scatter inelastically to create vibration quanta. This is a weak effect --approx. only 1 in 10⁶ of the incident photons is scattered to a wavelength that differs slightly from the incident wavelength.

- This is Raman scattering.



- The 90° Stokes Raman scattering intensity, expressed as the number of photons scattered per second is given by:

$$I_{fi}(\frac{\pi}{2}) = \left(\frac{\pi}{\epsilon_0}\right)^2 (\tilde{\nu}_0 \pm \tilde{\nu}_{fi})^4 J_0 \sum_{\rho, \sigma} [\alpha_{\rho\sigma}]_{fi} [\alpha_{\rho\sigma}]_{fi}^\dagger$$

- The intensity can be approximated with the Herzberg-Teller expansion as:

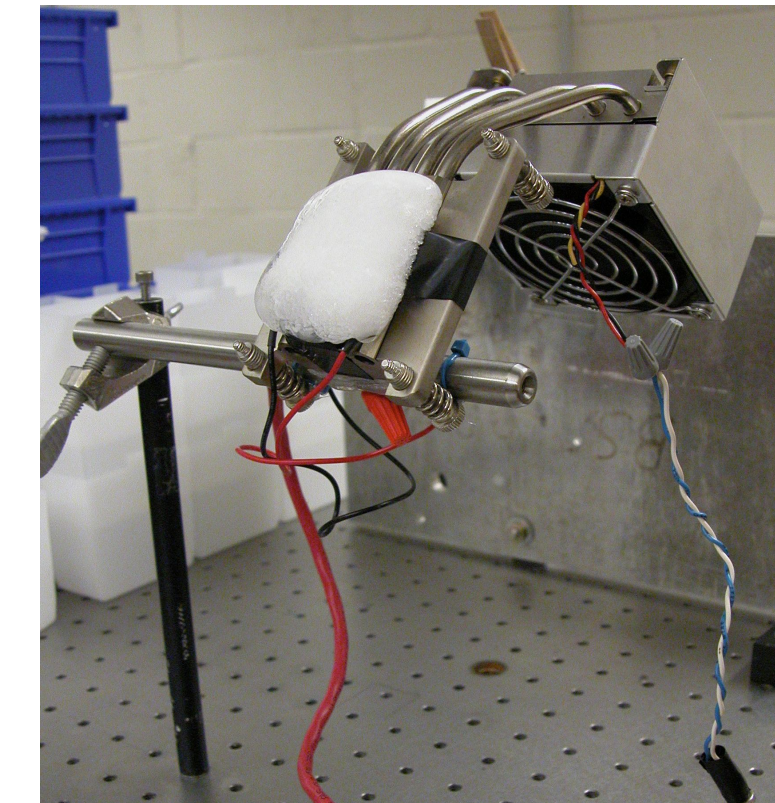
- Resonant Raman scattering can be modeled as $I_{fi}(\frac{\pi}{2}) = A + B + C + D$ as the incident wavelength falls within an electronic absorption band of the molecule, causing the vibrations of the absorbing specie to be enhanced.

- It is evident that the denominator in the first term can become very small when the incident laser radiation is close to that of an electronic transition, making the A term dominant. The A term:

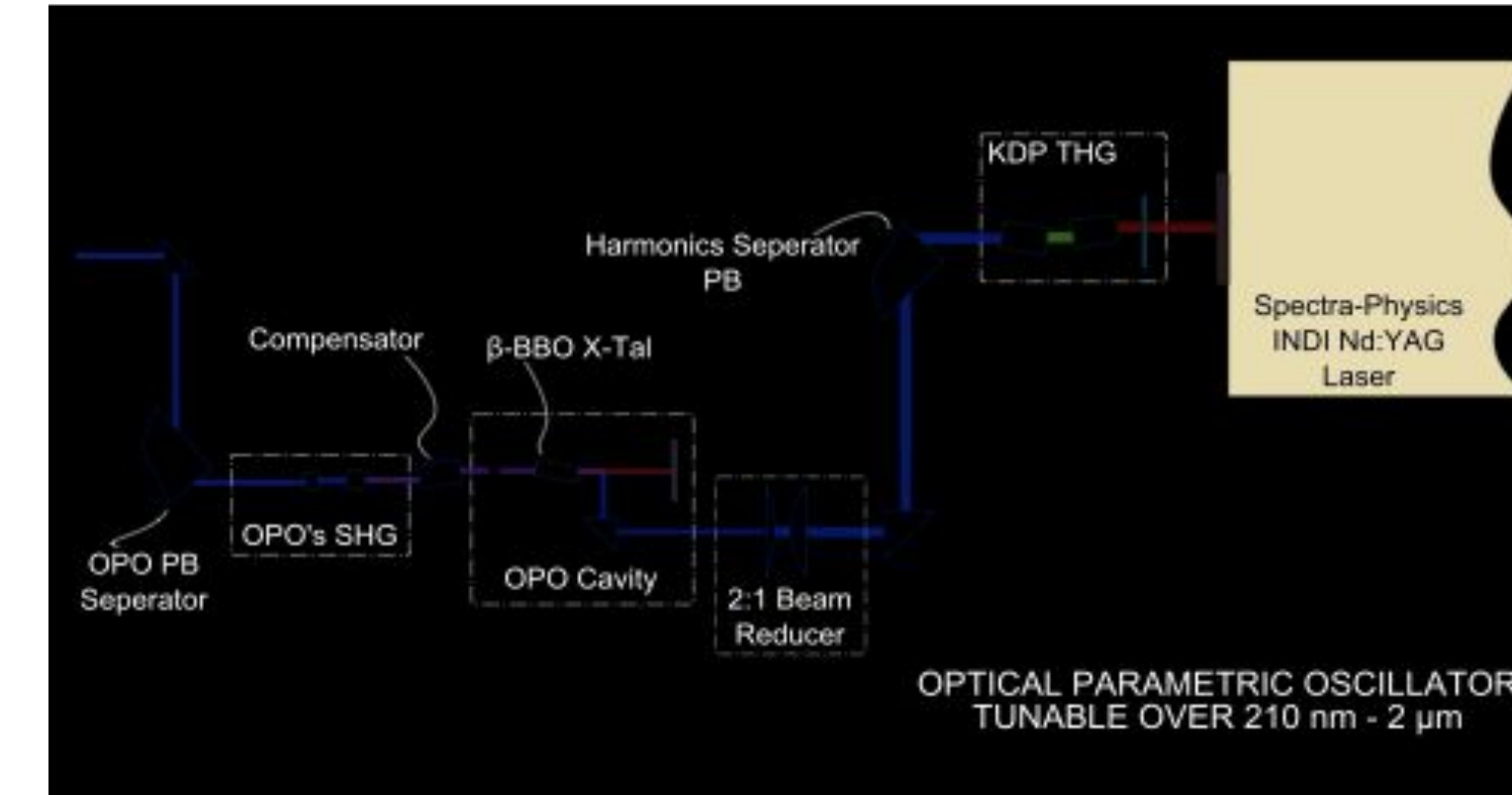
$$A = \frac{1}{\hbar c} [\mu_{\rho}]_{ge}^0 [\mu_{\sigma}]_{eg}^0 \sum_v \frac{\langle n_g | v_e \rangle \langle v_e | m_g \rangle}{\tilde{\nu}_{ev, gm} - \tilde{\nu}_0 + i\Gamma_{ev}}$$

Experimental Apparatus

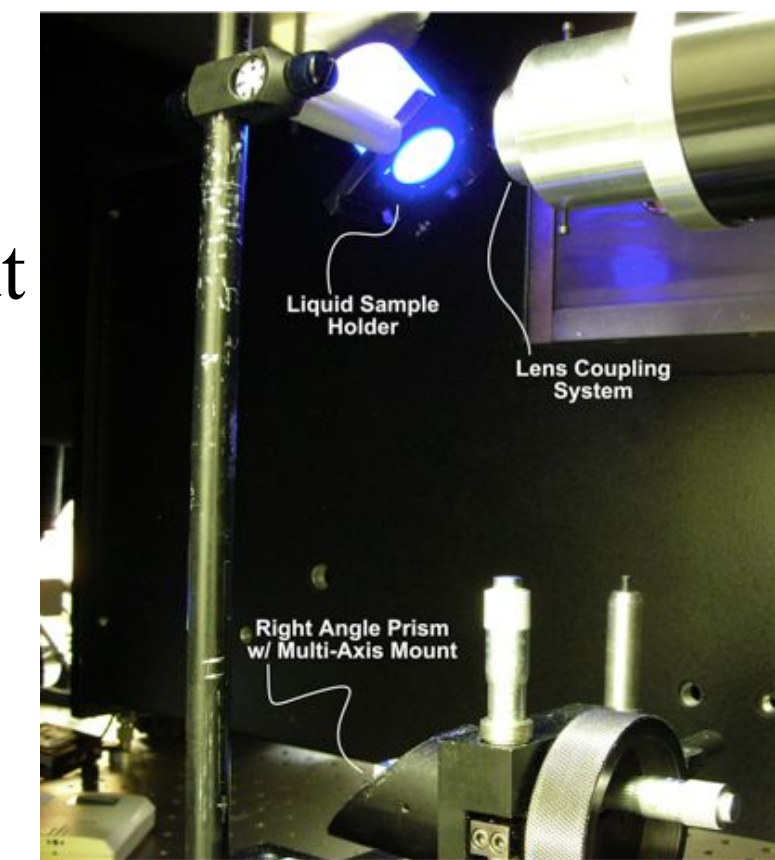
- To collect our data we used an optical parametric oscillator to create a tunable laser (215-700 nm), permitting studies around the absorption bands of various samples.
- A 90° optical scattering setup was utilized for collection of the Raman spectra.
- The Spex Triplemate 1877 three stage spectrometer spectrometer was utilized to filter out any stray light and Rayleigh scattering from the optical path.
- The spectrometer output was collected with an Andor EM-CCD camera.



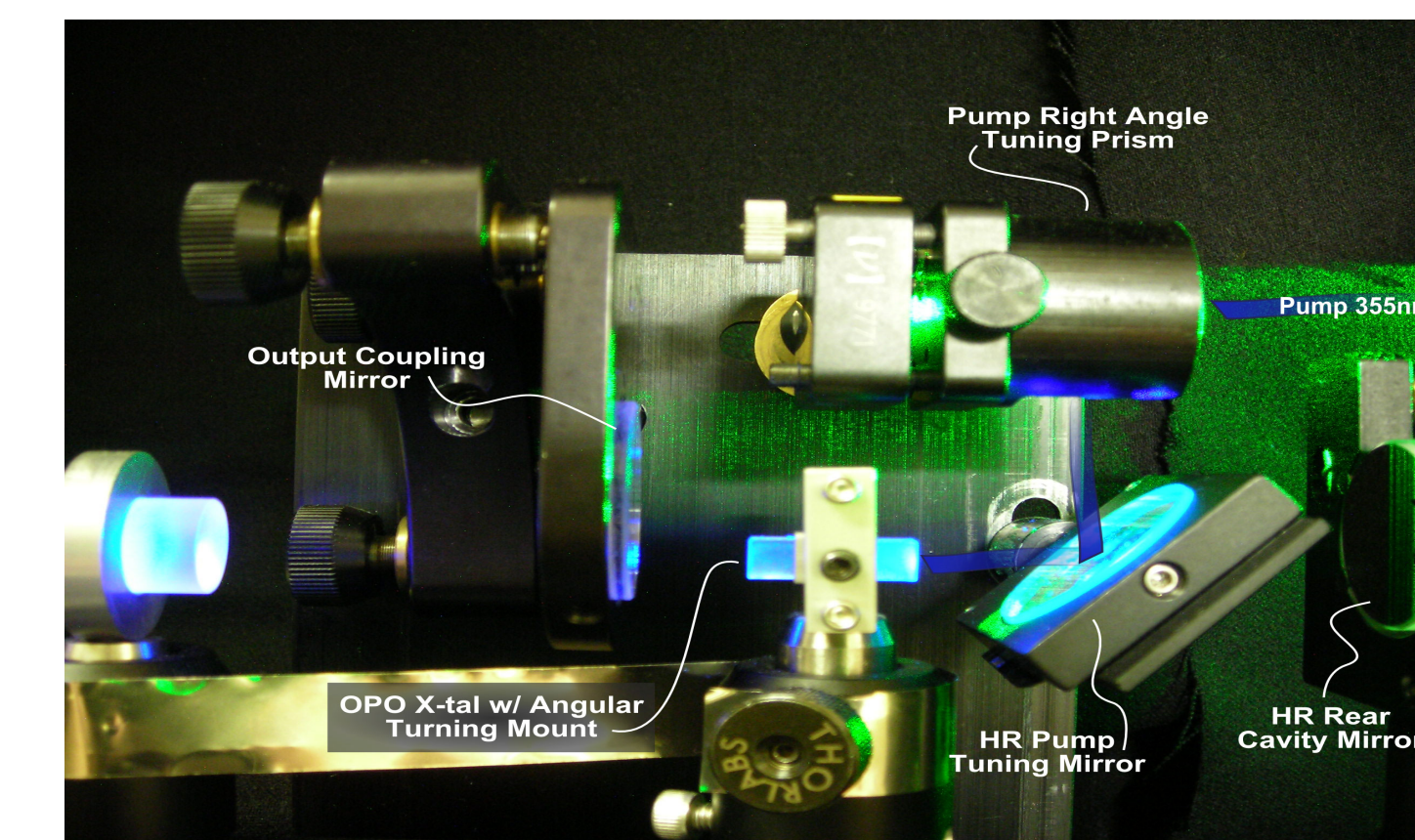
Peltier sample holder/collector.



Schematic of the tunable UV laser

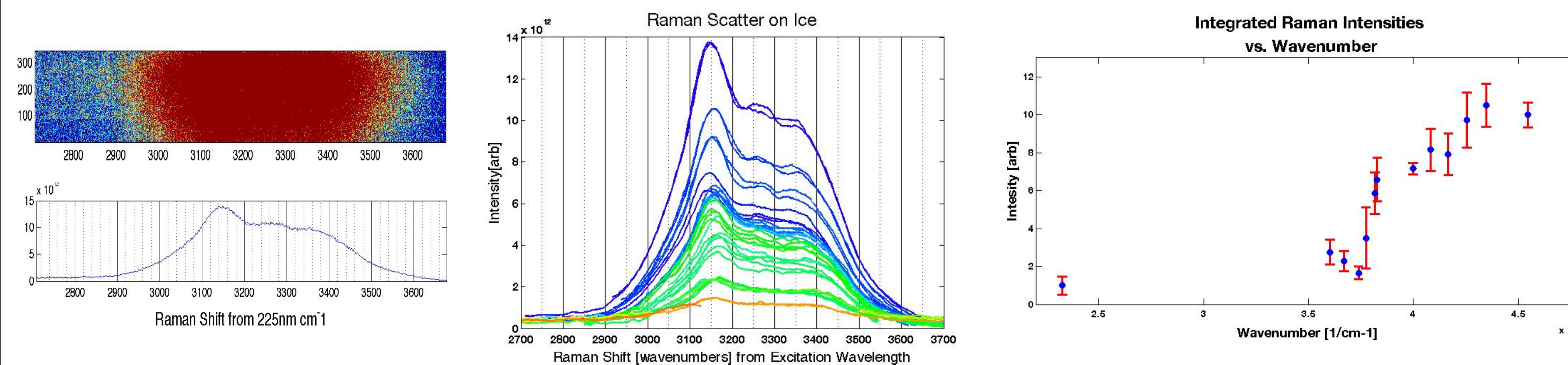


Spectrometer Input



Photograph of the OPO cavity

Results



- The output of the spectrometer is collected as an image. The vertical information reflects the sample position, and is integrated to obtain an average line spectra.
- Spectra for each image are seen above for incident wave lengths from 430nm to 221nm.
- The area under the Raman peak from each spectrum was normalized for laser power and the nonresonant ν_0^4 .

Analysis

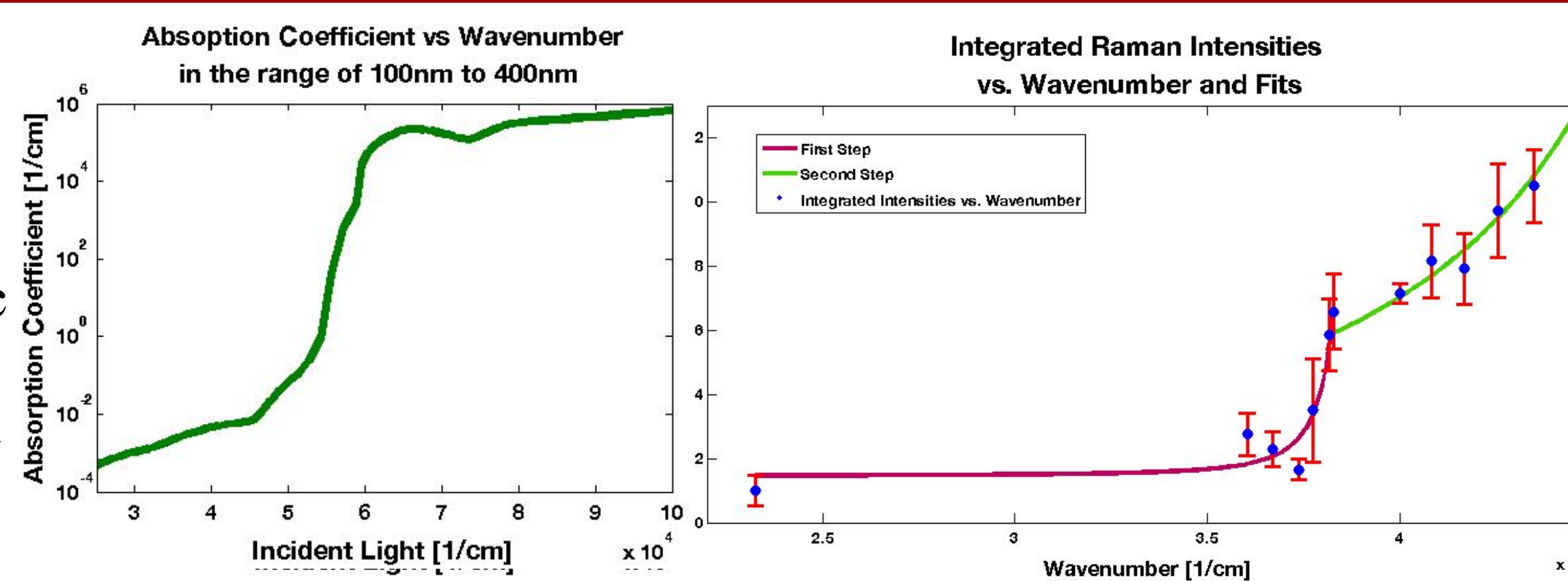
- Usually Raman scattering has an intensity proportional to ν_0^4 like dipole absorption/emission.
- A deviation from this proportionality occurs, due to the A term of the Raman scattering tensor, as the frequency of the incident light approaches an electronic transition.
- We take the derivative of the polarizability tensor with respect to the normal coordinate Q_a to obtain:

$$\partial(\alpha_{\rho\rho})_{kk}/\partial Q_a = A + B,$$

- Where: $A = \frac{1}{\hbar} \sum_r \left(\frac{2\nu_{rk}}{\nu_{rk}^2 - \nu_0^2} \right) \frac{\partial |(M_{\rho})_{rk}|^2}{\partial Q_a}$, $B = \frac{-2}{\hbar} \sum_r \frac{\nu_{rk}^2 + \nu_0^2}{(\nu_{rk}^2 - \nu_0^2)^2} |(M_{\rho})_{rk}|^2 \frac{\partial \nu_{rk}}{\partial Q_a}$
- From this we model our data, normalized and corrected for ν_0^4 , as proportional to the intensity of the A term. Our model takes the form:

$$I \propto C \left[\frac{2\nu_a^2}{(\nu_a^2 - \nu_0^2)^2} \right] + D$$

- Where C and D are proportionality constants and ν_a is the representative excitation frequency between the ground state and electronic state.



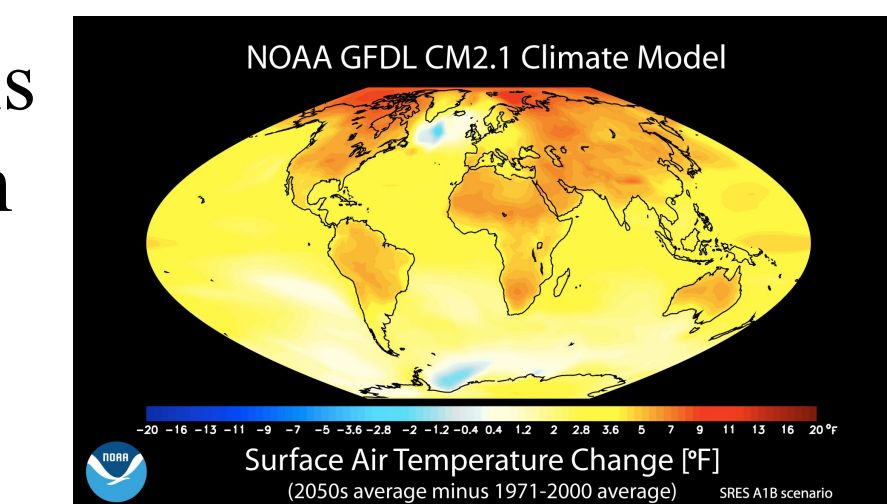
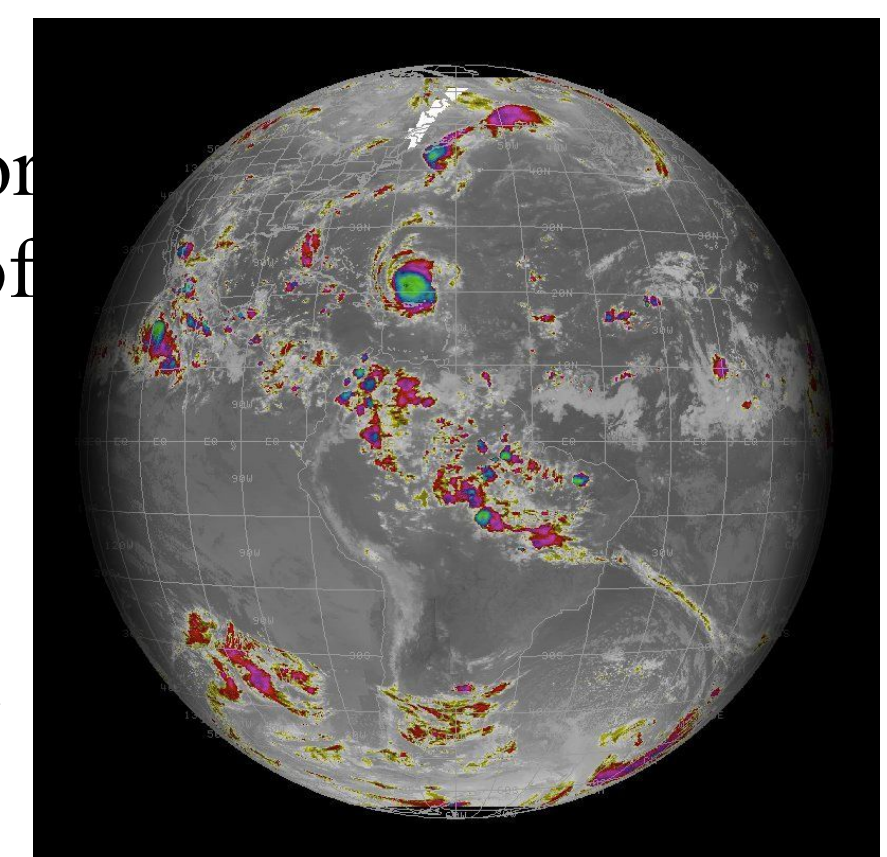
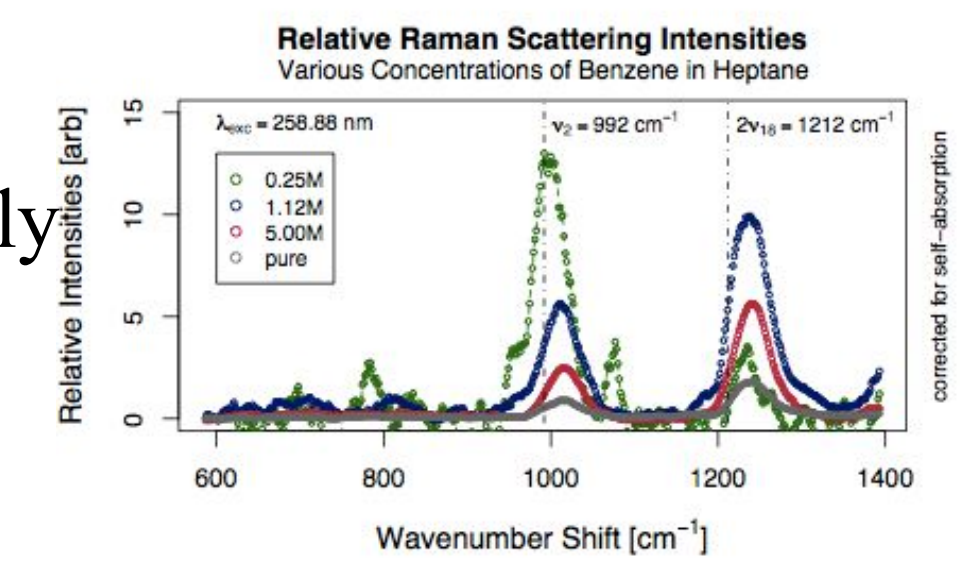
- The peaks on the absorption curve and the step-like increase at 3.8×10^4 wavenumbers suggests the resonant effect of two concurrent peaks.
- The first step resulted in $\nu_a = 256\text{nm}$ ($\chi^2 = .55$) and the second peak was found to correspond to $\nu_a = 180\text{nm}$ ($\chi^2 = 2.45$).
- These values correspond closely to the peaks in the absorption curve.

Conclusion

From these preliminary results, we find that the deep ultra-violet Raman scattering of ice is significantly enhanced compared to visible Raman scattering, by both non-resonant and resonant contributions. It is in agreement with a pre-resonant regime based on the implications of A term from the Raman scattering polarizability tensor.

Discussion

- In another investigation conducted with this study, (right) resonance Raman spectroscopy was found to only be effective in two circumstances: low sample volume or low sample concentration.
- These findings, particularly the strong enhancement observed for water, suggest that application of pre-resonant or resonant Raman LIDAR could vastly improve spatial and temporal resolution of water vapor measurements in clouds.
- Such data could be used as a key element in the measurement of energy flow at the cloud-air interface. This energy problem is one of the major uncertainties in current global climate models.



Selected References

Albrecht, A. C. (1961), 'On the Theory of Raman Intensities', The Journal of Chemical Physics 34(5), 1476-1484.
 Cotter, T. M.; Thomas, M. E. & Tropic, W. J. Palik, E. D., ed. (1991), Handbook of Optical Constants of Solids II, Academic Press, Inc., Orlando, Florida.
 Dudik, J. M.; Johnson, C. R. & Asher, S. A. (1985), 'UV resonance Raman studies of acetone, acetamide, and N-methylacetamide: models for the peptide bond', Journal of Physical Chemistry 89(18), 3805-3814.
 Gerrity, D. P.; Ziegler, L. D.; Kelly, P. B.; Desiderio, R. A. & Hudson, B. (1985), 'Ultraviolet resonance Raman spectroscopy of benzene vapor with 220-184 nm excitation', The Journal of Chemical Physics 83(7), 3209-3213.
 Hecht, E. (2002), Optics, Addison Wesley Longman, Inc., Reading, Massachusetts.
 Herzberg, G. (1966), Molecular Spectra and Molecular Structure, Vol. III. Electronic Spectra and Electronic Structure of Polyatomic Molecules, D. Van Nostrand Company, Inc., Princeton, New Jersey.
 Lee, S. (1983), 'Placzek-type polarizability tensors for Raman and resonance Raman scattering', J. Chem. Phys. 78(2), 723-734.
 Moore, J. H.; Davis, C. C. & Coplan, M. A. (1989), Building Scientific Apparatus: A practical guide to design and construction, Addison-Wesley, Inc., Redwood City, California.
 Rea, D. G. (1960), 'On the Theory of the Resonance Raman Effect', J. Mol. Spectrosc. 4, 499-506.
 D. J. Segelstein, "The complex refractive index of water," University of Missouri-Kansas City (1981).
 Whiteman, D. N.; Melfi, S. H. & Ferrare, R. A. (1992), 'Raman lidar system for the measurement of water vapor and aerosols in the Earth's atmosphere', Appl. Opt. 31(16), 3068.
 Ziegler, L. D. & Albrecht, A. C. (1979), 'Pre-resonance Raman scattering of overtones: The scattering of two overtones of benzene in the ultraviolet', J. Raman Spectrosc. 8(2), 73-80.
 Ziegler, L. D. & Hudson, B. (1981), 'Resonance Raman scattering of benzene and benzene with 212.8 nm excitation', The Journal of Chemical Physics 74(2), 982-992.

Acknowledgements

- Funding agencies: AFRL, NSF, ARO.
- Discussions: the other illustrious members of the NCSU Optics Group